Human Drivers based Active-Passive Model for Automated Lane Change

Quoc Huy Do, Hossein Tehrani, Seiichi Mita, Masumi Egawa, Kenji Muto, Keisuke Yoneda

***Abstract*— Lane change maneuver is a complicated maneuver that causes many severe expressway accidents. Automated lane change has great potentials to reduce the number of accidents. Previous research mostly tried to find an optimal trajectory and ignore the behavior model. To understand the human lane change model, we carried out experiments at Japan expressways. Through analyzing the human-driver lane change data, we proposed a two-segment lane change model to mimic the human-driver. We categorize the environment based on the observation grid and propose alternative behaviors to handle the complicated scenario. We develop an intuitive method to select the suitable lane change behavior including active (accelerate/decelerate) and passive (wait) based on distance and related velocity (dx/dv) graph. We also extracted the most preferable and safe condition for doing lane change based on the human driver preference data. We evaluated the proposed model by doing lane change simulations in PreScan environment with considering the vehicle motion/control model. The simulation results show the proposed model is able to handle the complicated lane change scenario and the performance is near the human driver.**

***Index Terms*— Automotive engineering, Navigation, Vehicle safety.**

I. Introduction

STATISCAL data of expressway traffic accidents shows that human error is a major reason for nearly 90% of accidents (Volvo 2013) [1]. Lane change maneuver is a cause for many severe expressway accidents due to wrong estimation of surrounding environment or wrong maneuvering. Currently, ADAS or automated driving has demonstrated the potential to reduce the impact of human errors. The literature in lane change or overtaking maneuver-based ADAS can be divided into rule-based [2], [3] or utility-based [4] approaches. In [5] and [6], Kasper et al introduced an object-oriented Bayesian network approach to model the traffic scene for the detection of lane change maneuvers. Bayesian network was also used by Schubert [7] for lane change situation assessment and decision making. In [8], the authors model the surrounding environment into an occupancy grid, then apply dynamic programing to find drivability cells and find proper decision for lane keeping or lane changing. Other related researches focus on maneuver prediction. In [9], [10] authors trained a neural network for the prediction of future lane change trajectory. A dynamic Bayesian network is also used by Gindele [11] and Schlechtriemen [12]-[13] for the behavior and trajectory prediction. Meanwhile, Kumar utilized the support vector machine and Bayesian filter for the same purpose [14]. The fuzzy logic was used by Naranjo et al [15] for modelling the lane change decision making. They use fuzzy controllers that mimic human behavior and reactions during overtaking maneuvers. Bahram [16] proposed a decision making based on a nonlinear model predictive approach. Mixed logical dynamical system is also used for solving lane change decision making as in [17]-[19]. Simon and Markus [20] applied an online Partially Observable Markov Decision Process to solve the decision making for lane change. Brechtel et al. [21] applied probabilistic MDP-Behavior planning for cars. Ardelt et al. [22] presented a probabilistic approach to build a lane change framework for automated vehicle. A lane selection method was proposed by Jin [23], however, this method requires all related vehicles connected. In [24], authors presented a collision avoidance method by analyzing the kinematic model of the vehicle and then calculated the minimum safety space requirement for performing the lane change. Other methods for lane change based on safety space checking are presented in [25], [26]. However, they provided a more general framework rather than focusing on lane change decision situations in particular.

The lane change trajectory is generated according to the vehicle state, surrounding vehicles and road information. The control laws are then designed to use on-board sensors to track the generated trajectory. Most of discussed researches either try to predict the behavior of surrounding vehicle or based on the kinematic functions and try to find an optimal trajectory or a safest path [27]-[29]. They ignore the ego vehicle lane change behavior model for complicated scenarios or in the presence of time/distance constraint for merging/exiting of the expressway. To exactly understand the human lane change model, we have conducted lane change experiments at expressways in Japan. The results of the human lane change motion analysis were already published by the authors [30]. By means of analyzing human lane change data including neighboring vehicles and motion/behavior data, we realized that the human model was

Q. H. Do and S. Mita are with the Research Center for Smart Vehicles, Toyota Technological Institute, Nagoya, Japan (e-mail: huydq@toyota-ti.ac.jp; smita@toyota-ti.ac.jp).

H. Tehrani, M. Egawa and K. Muto are with Corporate R&D Div.3, DENSO CORPORATION, Kariya, Aichi, Japan (e-mail: {hossein_tehrani, masumi_egawa, kenji_Muto}@ denso.co.jp) .

K. Yoneda was with the Research Center for Smart Vehicles,Toyota Technological Institute, Nagoya, Japan. Currently, he is with Autonomous Vehicle Research Unit of Institute for Frontier Science Initiative, Kanazawa University. (e-mail: k.yoneda@staff.kanazawa-u.ac.jp).

not a single stage. This paper is extended from our previous work [31]. In this paper, a multi-segment behavior and motion model to mimic the human-driver lane change operation is proposed. At the "behavior segment", the ego vehicle tries to adjust the longitudinal distance, position or relative velocity to make or find suitable free space in front of it and in the destination lane. Alternative behaviors for "behavior segment" are generated to be able to handle the lane change for any scenario. A method to select the suitable behavior based on the dx/dv graph segmentation is proposed. This graph provides the safety distance dx and safety speed dv for doing the lane change based on the human-driver lane change patterns.

At "motion segment", the ego vehicle starts lateral motion and enters into the destination lane. An optimization function is proposed which integrates both lateral and longitudinal trajectories in the same function. Through comparison with human-driver data, we found that the proposed evaluation function was able to select a motion close to human-driver.

The structure of this paper is as follows; Section II explains the analysis of human lane change data and our proposed automated lane change flowchart. Section III introduces our two segments lane change model and behavior generation and selection criteria. The lane change motion planning is also described in section III. Section IV presents our simulation and comparison results. Finally, the conclusion is given in section V.

II. Automated Lane Change Model

A. Lane Change Experiment

To evaluate the human driver motion during the lane change, we conducted experiments at Isewangan Expressway at Aichi prefecture. The experiment route with the length of 21.4 km is shown in Fig. 1(a) and marked inside red rectangle area. Different long-time-career expert drivers (whose driving skills are higher than average drivers) are selected for doing lane change experiments. Lane change maneuvers were frequently performed between different driving lanes to cover most possible scenarios in the expressway. The lane change experiments process utilized to record different human driver behavior and motion is shown in Fig. 1(b). When the driver receives request for changing the lane from test engineer, the driver adjusts the longitudinal speed (acceleration/deceleration) and finds a safe space and time instant to start steering for lane change. Lane change in expressway is generally a challenging task, and the driver should adjust both the lateral and longitudinal acceleration to perform safe and comfortable lane change. All the surrounding vehicles' information, including their relative distance, and speed, was also extracted. These data are used to analyze the human driver behavior during the lane change. Figure 1(c) shows the diagram of the whole lane change experiment to extract data and evaluate the proposed lane change method.

B. Lane Change Model

Through lane change experiments, we learned that the human-driver model does not begin at the instant of the steering

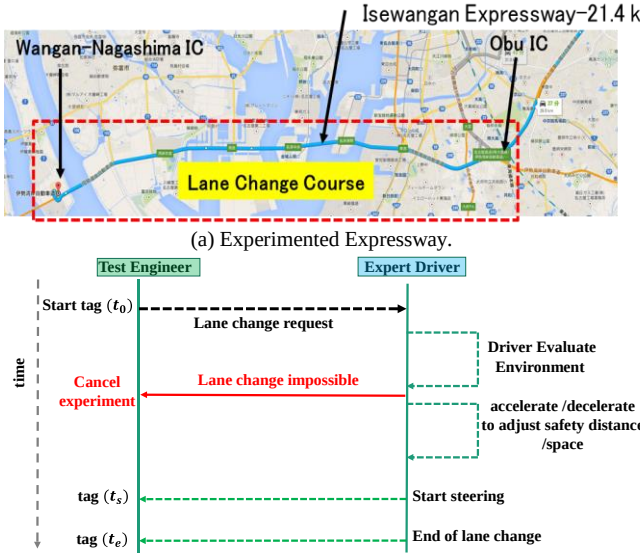

(a) Experimented Expressway.

(b) Lane change experiments process to extract the human driver behavior.

(c) Lane change experiment diagram.

Fig. 1. Lane Change experiment.

wheel turn, but rather several seconds before the steering wheel turn. Figure 2 (a) shows an example of a recorded lane change scenario. The ego vehicle (red car) wanted to change to the right lane. However, there was one vehicle ahead of the ego-vehicle and one vehicle coming from behind in the intended target lane. As shown in sample in Fig. 2 (a), turning the steering wheel starts at time 17, although the human-driver has already started to decelerate and reduce the vehicle speed from 23.85 m/s to 22.23 m/s. The driver had to decelerate to keep safe space from the front vehicle and wait for the vehicle coming from behind in the right lane to pass before starting the lane change. In this paper, a two-segment behavior/motion lane change model is proposed as shown in Fig. 2 (b). In segment 1, "behavior segment", the ego vehicle tries to adjust the longitudinal distance, position or relative velocity to make or find suitable free space in front of it and in the destination lane. In segment 2, "motion segment", the ego vehicle starts lateral motion and enters into the destination lane. The driver behavior in segment 1 is highly dependent on the number of surrounding vehicles, distances and their relative velocities. When the vehicles enter/exit from an adjacent lane to the mainstream

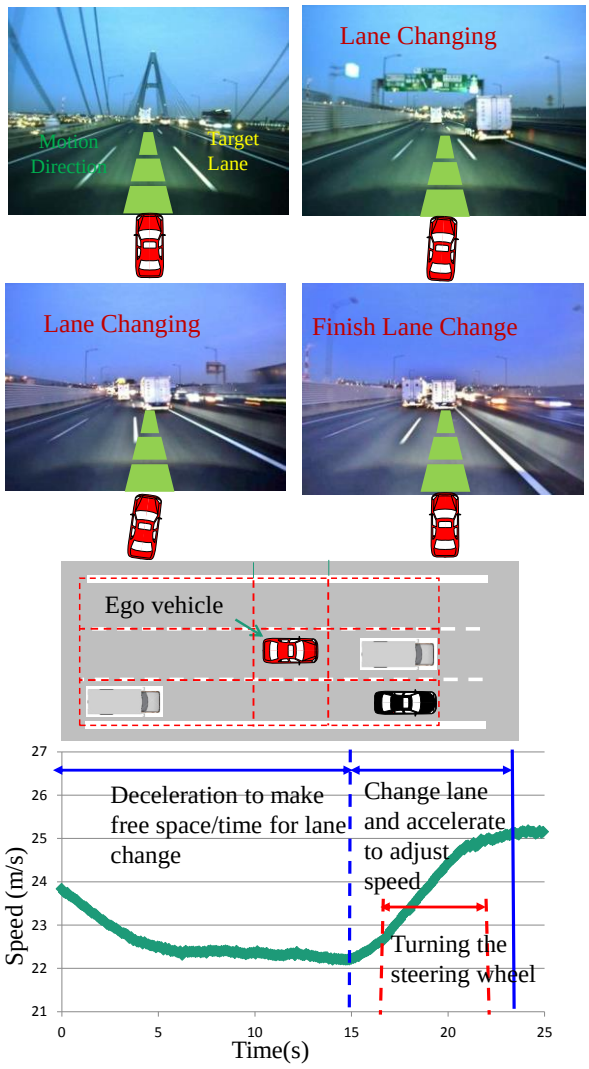

a) Lane change scenario.

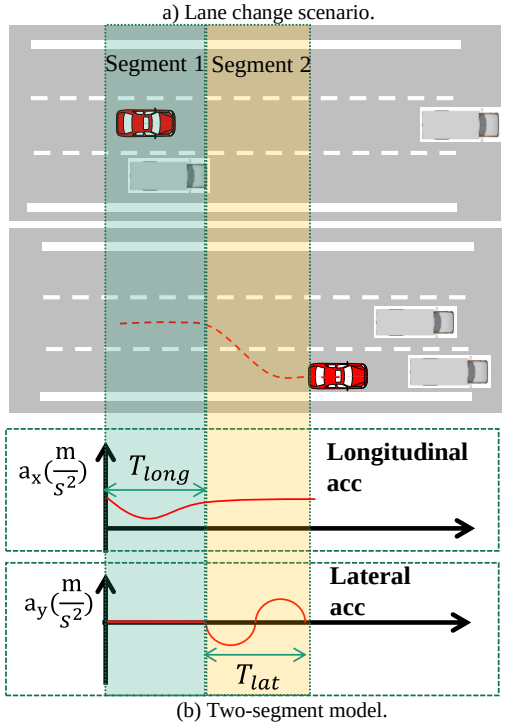

(b) Two-segment model.

Fig. 2. Two-segment lane change model.

traffic, the time/distance constraint is also a critical factor to select the suitable behavior at segment 1. This factor is based on the specific length of the adjacent road. There are also other important parameters such as road curvature, visibility condition or behavior of the surrounding vehicles. By analyzing different cases of human lane change data, the following behaviors for the segment 1 are extracted.

$$B = \{do\ lane\ change(LC), passive(wait), active(accelerate), active(decelerate), active(evasive)\} \quad (1)$$

Although it is difficult to develop a general behavior model, it is possible to propose a standard model that guarantees the safety and smoothness of the lane change operation. For example, if there is enough space at the destination lane, the vehicle can turn the steering wheel and ***do the lane change***. If the relative speed of the approaching vehicles in the destination lane is relatively high, ego vehicle may prefer to ***wait*** *(passive)* until finding enough free space. In this case, it may even do ***deceleration*** *(active)* to reduce the time or traveled distance. The deceleration behavior may be useful in the case of time/distance constraint when ego vehicle has to change the lane to exit from the expressway. In the other case, when the relative speed of the neighboring vehicles in the destination lane is relatively low, ego vehicle may ***accelerate*** *(active)* to pass the neighboring vehicles for doing the lane change. If there is a sudden change in the behavior of the surrounding vehicles during the lane change (sudden acceleration, deceleration or lane change), ego vehicle might need ***evasive*** *(active)* maneuver to avoid accident. On the other hand, the road curvature, speed

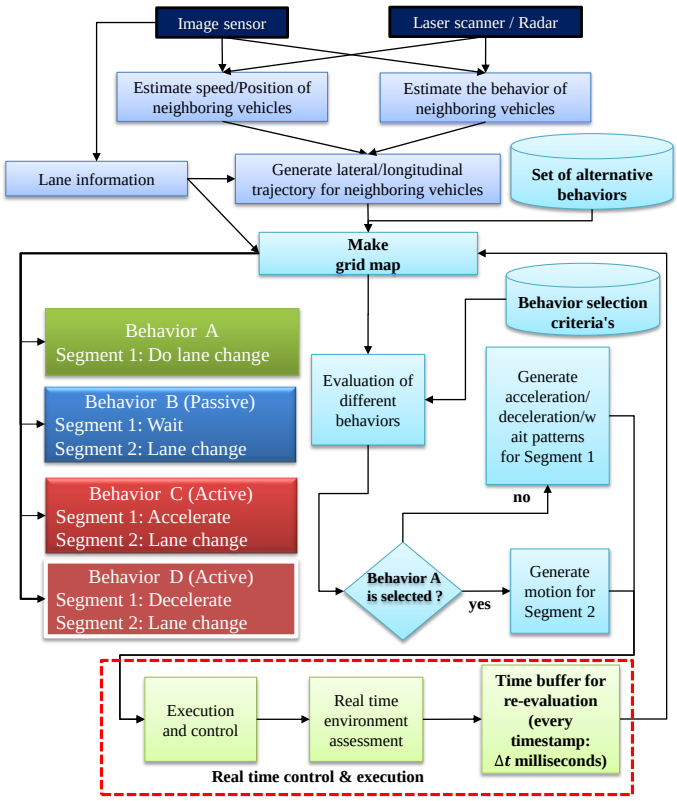

Fig. 3. Automated lane change flowchart.

limits and kinematic constraints of the vehicles such as maximum speed or acceleration also have impact on the driver's behavior.

C. Automated Lane Change Flowchart

Automated lane change is an integration of sensing/perception, planning (behavior & motion) and control. The behavior/motion flowchart for doing the lane change is shown in Fig. 3. It starts with estimation of motion parameters/ position of neighboring vehicles to estimate their trajectories. Based on the driving lane information and the behavior/motion parameters of the neighboring vehicles, a trajectory for a certain period $[0{\sim}T]$ can be estimated. By using the trajectory data points $(t, x(t), y(t))$, the occupancy grid map of current and future state of the surrounding environment is estimated. In the following, the main components of the automated lane change flowchart are briefly explained.

D. Situation Modelling

The current lane change situation is modelled into a state occupancy grid as in the Fig. 4. This state grid is attached to the vehicle position. The grid cell's width and orientation are equal to the lane width. The middle cell length d_{ego} is equal to the ego vehicle length plus a safety distance. The grid's size is calculated based on the relative velocity of the ego vehicle and surrounding vehicles, and the time to complete the lane change. The front cell size's d_{front} is calculated based on the closest vehicle in the front, and behind cell's size d_{back} is calculated based on the corresponding closest vehicle approaching from behind.

$$d_{front} = d_{min} + \max\{v_{ego} - v_{front}, 0\} * Time_{LC} \quad (2)$$

$$d_{back} = d'_{min} + \max\{v_{back} - v_{ego}, 0\} * Time_{LC} \quad (3)$$

$Time_{LC}$ is the intended or required time to perform lane change maneuver, and it takes 4–6 s for a typical driver to complete lane change and based on human driver data [32]. v_{front} is the velocity of the closest vehicle in the front, and v_{back} is the velocity of the closest vehicle behind the ego vehicle; d_{min} and d'_{min} are human defined minimum safety distances; v_{ego} is the current ego vehicle's velocity. In literature, the grid cells are generally considered to be same size [5],[8]. Empirically through simulations and recorded human-driver data, we realized that the center cells in the grid were just dependent on the vehicle size and they were generally smaller than the front and back cells in the grid. Considering large size for center cell causes the ego vehicle does not do the lane change due to occupation of the center cell in the left or right side. We also realized that the back cells have larger size compared to front cells to mimic the human behavior.

By discretizing the surrounding environment into a nine-cell grid, it is possible to present different states to perform the lane change. There are eight surrounding cells in the occupancy grid and each cell can be either free (cell value = 0) or occupied (cell value = 1). Thus there are totally 2^8 = 256 states. Since the vehicle only perform either the left side or right side lane change maneuver, the other side's cell can be temporarily ignored so that the number of state can be reduced to 2^5 = 32 states.

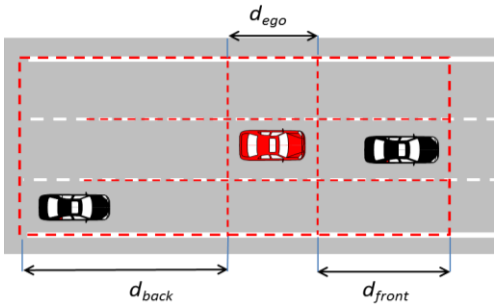

Fig. 4. Environment grid modelling.

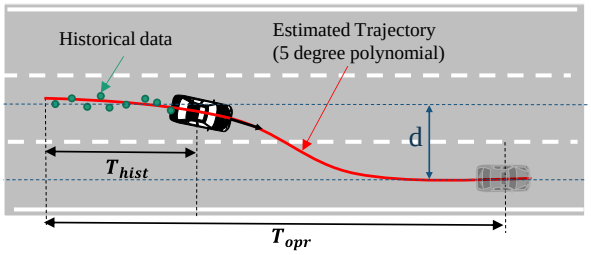

Fig. 5. Neighboring vehicle's trajectory estimation.

E. Trajectory Estimation of Neighboring Vehicles

Recorded past motion data, road information and behavior (lane change/lane keeping) are utilized to estimate the trajectory of the neighboring vehicles. Polynomial function is used to estimate the trajectory of the neighboring vehicles [33]. As shown in Fig. 5, the trajectory of a neighboring vehicle is estimated by recorded position data and lane center point (we assume that this vehicle will follow the center of the lane) and a polynomial curve is fitted to these data. Quintic polynomials are used to generate the estimated trajectory. This is given as

$$y(t) = a_5 t^5 + a_4 t^4 + a_3 t^3 + a_2 t^2 + a_1 t + a_0 \quad (4)$$

$a_i (i = [1,4])$ is polynomial function's factor which can be calculated based on the past motion data point and the lane center points.

T_{hist} is recorded time and T_{opr} is total operation/prediction time. Here, "Frenet Frame" method is applied in order to combine different lateral and longitudinal motions in one equation [33]. In this case, the lateral and longitudinal motion of each vehicle can be presented by an equation which is based on the distance traveled along the center line.

There are effective collisions checking methods in the literature to check the collision between two trajectories [34]. To check the collision in the simulation platform, the trajectory of the neighboring vehicle is sampled for a certain period [0~T]. Inevitable Collision States (ICS) method [35] is applied to check the collision possibility between two trajectories.

III. Behavior and Motion Generation

A general two-segment model for doing lane change has been already proposed in previous section. At segment one, "*behavior segment*", the ego vehicle tries to adjust the longitudinal relative distance, velocity to make or find suitable free space in front or in the destination lane. In this segment, the ego vehicle may accelerate, decelerate or just wait to make free space/time interval at the destination lane. At segment 2,

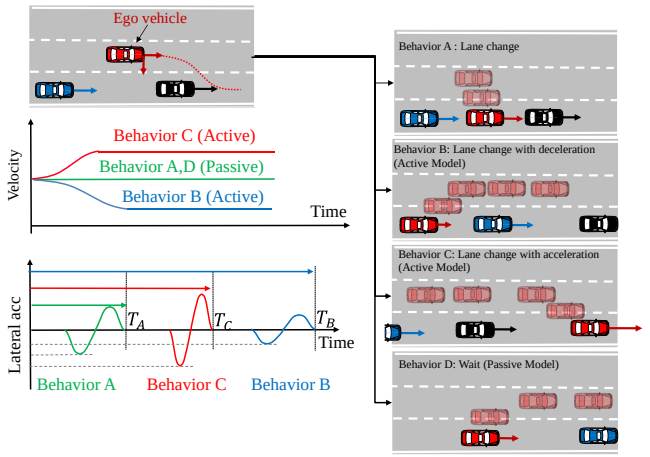

Fig. 6. Different available behavior and motion for lane change and velocity profile corresponding to each behavior.

"*motion segment*", the ego vehicle starts lateral/longitudinal motion and enters the destination lane.

This paper extends "behavior segment" introduced in [36] and briefly review the lateral/longitudinal motion generation method for "motion segment" presented in [29].

A. Behavior Segment

For every state, different alternative behaviors are considered as shown in Fig. 6. For the situation in Fig. 6, different following behaviors are available to do the lane change;

- Behavior A: The ego vehicle does the lane change with current speed as there is enough space and the relative velocities of the vehicles in the right lane are not high.
- Behavior B (active): The ego vehicle decelerates and enters to the right lane at the back of the vehicles. It is preferable behavior when the lane change at limited time/distance has to be done (for example exit point in the expressway).
- Behavior C (active): The ego vehicle accelerates and enters to the right lane at the front of vehicles.
- Behavior D (passive): If the relative speeds of right lane vehicles are high, the ego vehicle just waits until the right lane vehicles passes and the right lane becomes free to do right lane change.

The proper behavior can be selected based on the relative distance and between the ego vehicle and neighboring vehicles. The large of difference of relative velocity are shown in the graph in Fig. 6 which was extracted from recorded human-data. To have exact understanding of different behaviors, we categorized 32 (2^5) occupancy gird states (left or right lane change) to the following four main categories. The behavior alternatives are limited based on the categories to reduce the calculation time. Different categories for occupancy grid states are shown in Fig. 7. In Fig.7, the white cells are empty cells, light gray cells are temporarily not considered cells due to the direction of the lane change and black cells are occupied cells. The categories and alternative behaviors are defined based on our experiments from analyzing the human-driver data for different lane change scenarios.

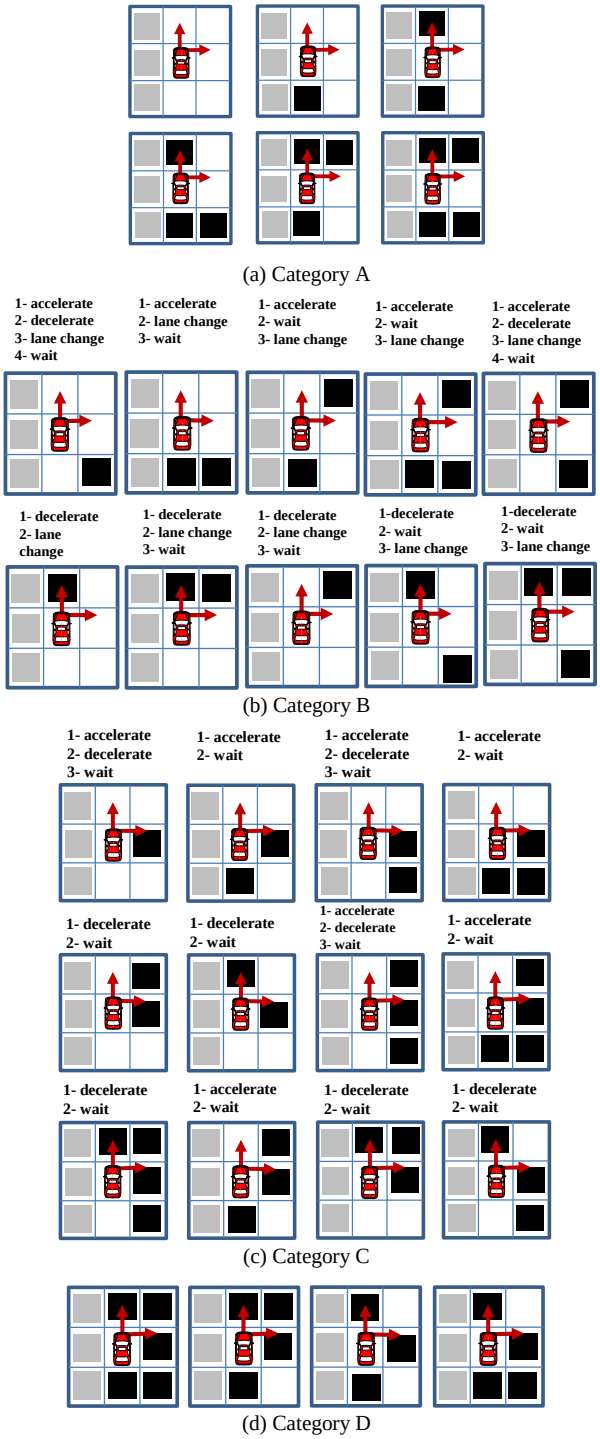

Fig. 7. All 32 states models for right lane change and available alternative behaviors for each of them.

- **Category A:** There are two alternative behaviors for occupancy grid states. The ego vehicle either waits or performs the lane change based on the relative speed and distance to the neighboring vehicles.
- **Category B:** There are more alternative behaviors for states in this category. The ego vehicle may do the lane change but sometimes acceleration/deceleration or wait is

preferable to do safer/smoother lane change. In the case of time/distance constraint, acceleration/deceleration may be necessary to satisfy the lane change limitations.

- **Category C:** It is related to complicated state during lane change. In this category, the right cell of the ego vehicle is occupied and suitable behavior should be selected to provide free space at the destination lane. Ego vehicle may accelerate, decelerate or wait for states in this category.
- **Category D:** The ego vehicle has to wait for doing the lane change and any other behavior may be dangerous.

The observation grid state can transit from one category to another depending on the driver and neighboring vehicles. The human driver often draw the current situation in his brain and match it with the four categories and figures out which situation is next if he selects a specific behavior. Eventually, category A is selected by accelerating or decelerating the vehicle, and lane change maneuver is initiated.

B. Behavior Selection

To select the suitable behavior for lane changing, there are many researches in the literature that are mainly based on HMM [37] or Bayesian network [27]. In this section, an intuitive method to extract the behavior patterns from the human-driver recorded data is proposed. The dx/dv graph is drawn for all the recorded lane change data from start t_0 until end of the lane change at t_e. The dx/dv is calculated when the ego vehicle driver decides to do the lane change in the presence of the vehicle in the destination lane. This graph corresponds to the "behavior segment" in proposed lane change model. Each draw includes the (dx, dv) status for the "behavior segment" while the driver adjusts the longitudinal distance/speed to make the safe space and time before the steering at t_s. An example of dx/dv for human driver regarding to a typical right lane change scenario is shown in Fig. 8. The horizontal axis is the related distance dx between vehicle in the target lane and the ego vehicle, and vertical axis is the velocity difference dv between two vehicles. In Fig. 8, the human driver slowly accelerates (active) until the neighboring vehicle in the right lane passes. (dx, dv) points are shown in Fig 8 and there are noises due to the sensor noise and detection/tracking uncertainties, the (dx, dv) points are not smooth or linearly continuous. To handle the sensor uncertainty and noise, we consider a margin for the (dx, dv) data and interpolate a line to model the human driver behavior.

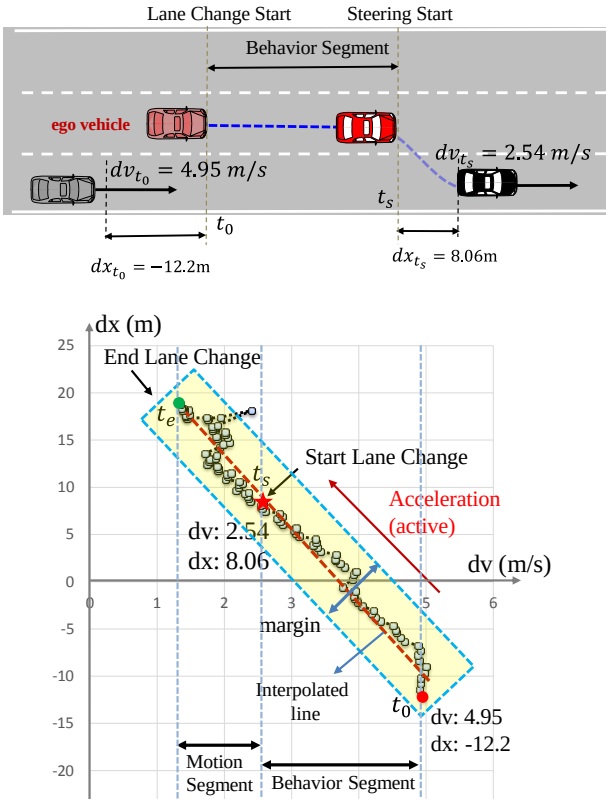

Fig 8. dx/dv graph for human right lane change.

More than 90 cases of human driver lane change were analyzed, and dx/dv graphs for all these cases were drawn. The dx/dv graph for right lane change cases is shown in Fig. 9. The horizontal axis is the distance between vehicle in the target lane and the ego vehicle, and vertical axis is the relative velocity between two vehicles. The lines show different recorded right lane change data that start from t_0 (human-driver decide to do the right lane change) until the t_s (red star) that driver steers to enter the right lane and continue. Based on the different samples of human-driver that are shown in Fig. 9, the dx/dv graph's area is able to be divided into three areas corresponding to three different behaviors including $lane\ change$, $accelerate\ (active)$ and $wait (passive)$ based on the initial value for (dx, dv). At the start of the right lane change, if the corresponding (dx, dv) point is in "Lane Change" area, the ego vehicle is able to enter to right lane. If the (dx, dv) is in "Wait" (passive) area, ego vehicle waits until (dx, dv) enters the "Lane Change" area (the right vehicle pass) and then enters to the right lane. If the (dx, dv) is in "Accelerate" (active) area, ego vehicle will accelerate and wait until (dx, dv) value enters the "Lane Change" and then do the lane change. The acceleration behavior is usual because the ego vehicle enters the higher speed lane and it should adjust speed with current lane. This graph also shows the safety relative distance dx or relative speed dv for doing the safe and comfortable right lane change. For sample LC_{001} in Fig. 9, the driver accelerates and reduces its relative speed before enter to the right lane. For sample LC_{002}, the driver waits until the right lane vehicle passes it and then starts to enter to the lane change.

The dx/dv graph in Fig.9, is only prepared for the positive values of dv because all the human lane change data lie in this area and vehicles in the right lane have generally higher speed. To complete the graph and cover all the values of dv, it is necessary to provide the human driver lane change data for the negative values of dv.

The dx/dv graph for the typical left lane change cases in expressway was also prepared. As shown in Fig. 10, the driver behavior is different from the right lane change because in this case, the vehicle enters to the lower speed lane. Similarly, the dx/dv graph area can be divided into three areas

corresponding to three different behaviors including $lane\ change$, $decelerate\ (active)$ and $wait (passive)$ based on the initial value of (dx, dv).

The dx/dv graphs in Fig. 9 and 10 provide an intuitive model for performing safe and comfortable lane change. Based on the initial value of (dx, dv), we are able to select the suitable active/passive behaviors and generate speed and timing profile for doing the automated lane change. As shown in Fig. 11, there is a vehicle in the right lane and we are initiating the right lane change with initial condition at (dx_{t_0}, dv_{t_0}). , There are many alternatives as shown by different lines from No. 1 to No. 5 for doing the lane change. For example, case No.1, we just wait in the (passive mode) until the back vehicle in the right lane passes. For other cases (active model), we accelerate to reduce our relative speed.

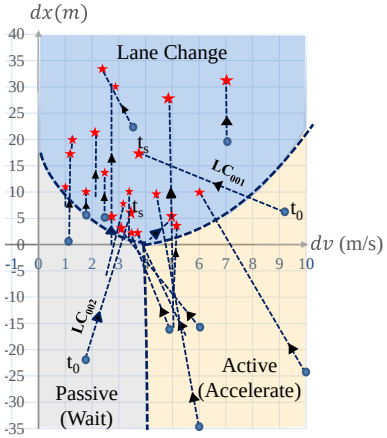

Fig. 9. dx/dv graph related to human driver behavior for doing the right lane change.

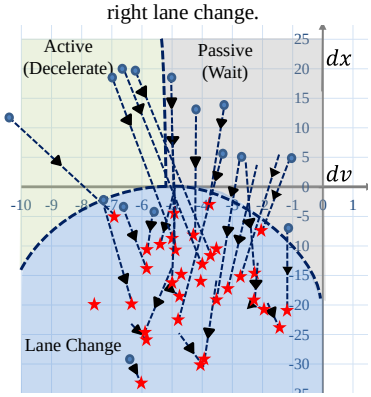

Fig. 10. dx/dv graph related to human driver behavior for doing the left lane change scenario.

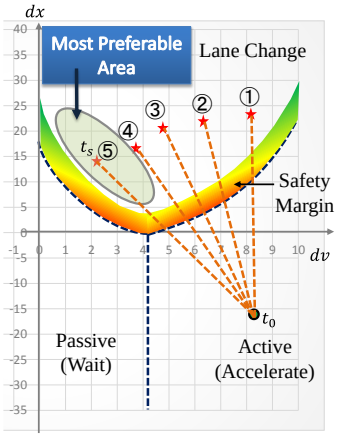

Fig. 11. Selection of suitable behavior pattern based on the initial value of (dv, dx) for right lane change

If we carefully look at the human lane change data in Fig. 9, there is an area, where most of the human lane change begins. This area is named as the "most preferable area". In the "most preferable area", the relative velocities dv is between [0 ~ 3 m/s] and relative distance dx is between [5 ~ 20 m]. To select the human like behavior for doing the right lane change, we draw the shortest line from initial condition at (dx_{t_0}, dv_{t_0}) to "most preferable area" and generate speed profile and lane change timing. We track the (dx, dv) and when we enter into the "most preferable area"; we start to do the lane change. One advantage of our approach in comparison with other related method is the calculation time. Since all the data are recorded and processed off-line to generate the dv-dx graph. The behavior selection is simplified into matching the current (dv-dv) point into the graph so that the calculation time is small (less than 10 ms).

C. Velocity Profile Planning (Behavior Segment)

According to the active/passive behavior, the corresponding desired vehicle's velocity profile is calculated. The acceleration/deceleration patterns are presented in the form of a function of ego vehicle position, velocity and the target leading/behind vehicle.

Figure 12 illustrates the vehicle acceleration behavior when a leading vehicle exists in the neighboring lane. In this scenario, ego vehicle accelerates and passes the leading vehicle. The acceleration is continued till sufficient safe distance is achieved, before performing the lane change maneuver. The ego vehicle's acceleration is calculated based on (5):

$$\ddot{x} = \frac{2\left(x_{lead}(t_0) - x(t_0) + T\left(v_{lead}(t_0) - v(t_0)\right) + r\right)}{T^2} \quad (5)$$

where $x(t_0)$: vehicle position at time t_0;
$v(t_0)$: velocity at time t_0;
$x_{lead}(t_0)$: leading vehicle position at time t_0;
$v_{lead}(t_0)$: leading vehicle position at time t_0;
T: operation time horizon;
r: safety reserving distance;

r is calculated through leading vehicle velocity and time to react TTR

$$r = d_{min} + v_{lead}(T) * TTR \quad (6)$$

To generate smooth and comfort acceleration/deceleration motion, the following cost function is minimized;

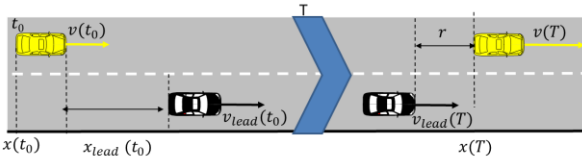

Fig. 12. Vehicle acceleration for passing.

$$J = \int_0^T (\omega_{dist}\,[\Delta d(t)]^2 + \omega_{acc}[\ddot{x}(t)]^2)dt \quad (7)$$

where ω_{dist} and ω_{acc} are human given weighted factor to balance between the jerk and safety distance (Δd). This cost function is similar to the method presented in [20] though the operation time T is fixed in [20]. In our approach, the operation time T is not fixed to have more degree of freedom. The error in the safety distance $(\Delta d(t))$ is calculated by the following;

$$\Delta d(t) = x_{lead}(t) - r + t * \dot{x}_{lead}(t) - x(t) \quad (8)$$

There is direct method to solve the above problem using Lagrange multiplier and Gradient Descent. Though finding the exact solution for optimization problem in (7) is difficult and time consuming. Here, we turn our attention to approximations of the minimizer through a simplification and sampling from search space. Instead of calculating the best trajectory explicitly and modifying the coefficients to get a valid alternative, we generate in a first step, such as in [33, 38], alternative trajectories for both $x(t), y(t)$. Later we can pick the valid and safe motion which is safe and has the lowest cost value.

The quartic polynomial function is utilized to generate acceleration/deceleration motion [34].

$$x(\mathrm{t}) = b_4t^4 + b_3t^3 + b_2t^2 + b_1t + b_0 \quad (9)$$

The coefficients $b_i(i = [1,4])$are estimated by considering ego vehicle constraints (maximum acceleration/deceleration and speed), operation time (T) and desired velocity at the end $\dot{x}$(T). Alternative longitudinal trajectories are generated by sampling a valid range of operation time T and final velocity $\dot{x}$(T) (it can be extracted from dx/dv graphs) while considering the boundary conditions including maximum and minimum acceleration $\ddot{x}_{max}, \ddot{x}_{min}$. We generate alternative speed profiles by sampling and select the best speed profile which has the lowest value for cost function in (7).

D. Motion Segment

To model a lateral path during a lane change, many approaches in literature use 5th degree polynomials as it provides minimum jerk for steering [27, 37]. Polynomial function provides a geometric modelling of the vehicle trajectory that responds to the realistic demands of the lane change maneuver.

$$\mathrm{y(t)} = a_5t^5 + a_4t^4 + a_3t^3 + a_2t^2 + a_1t + a_0 \quad (10)$$

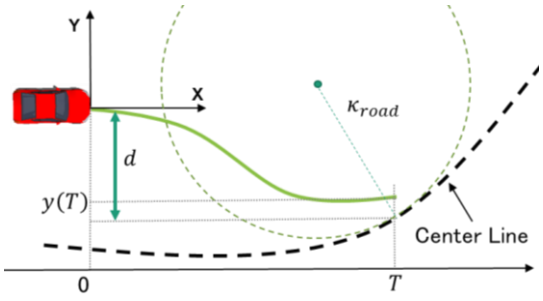

Fig. 13. Lateral trajectory optimization.

The equation coefficients $a_i(i = \overline{0,4})$ are calculated considering dynamic constraints (boundary conditions for lateral acceleration) and values of the position, velocity and acceleration at initial and endpoint. The initial velocity and acceleration of vehicle can be obtained from the CAN and generate alternative lateral trajectories by changing operation time T. T is sampled from a valid range of operation time and ending conditions to generate alternative lateral trajectories while considering the boundary conditions including $\ddot{y}_{max}, \ddot{y}_{min}$ and $\kappa(t) \leq \frac{\ddot{y}_{max}}{\dot{x}(t)^2}$ to avoid slip. The best lateral motion is selected which minimize the following cost function that includes lateral jerk, heading error and smoothness as shown in Fig. 13;

$$J = w_{jerk}\int_0^T \dddot{y}^2(t) + w_{heading}[\kappa(T) - \kappa_{road}]^2 + w_{smoothness}\int_0^T \frac{\dot{\kappa}(t)^2}{\sqrt{\dot{x}(t)^2 + \dot{y}(t)^2}} \quad (11)$$

where w_{jerk}, $w_{heading}$ and $w_{smoothness}$ are human given weighted factors.

IV. Simulation

To evaluate and test the proposed model, a simulation platform on the Prescan was developed. It includes different modules for sensing, behavior/motion planning, trajectory estimation of neighboring vehicles and ego vehicle's control. The behavior/motion generation module is developed under C++ to increase the efficiency of the simulation platform.

A. Lane Change Scenario

Figure 14 shows simulation results for the right lane change scenario with different relative speed (dv) for neighboring vehicles (ego vehicle is red one and it is going to do right lane change). In Fig. 14, the ego vehicle (red vehicle in the central lane) wants to perform the lane change maneuver to the right-side lane with initial $(dx_{t_0} = -25m\,, dv_{t_0} = 7.3\,m/s)$. Based on the proposed method, the ego vehicle makes a speed and timing profile to the "*most preferable area*" as shown by dotted red line in Fig. 15. It slowly accelerates (active model) and starts the lane change when enter to the safe area as shown in Fig. 14 simulation. We have tested the

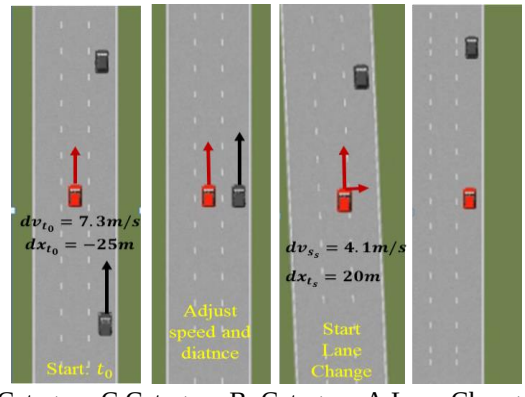

Category C Category B Category A Lane Change

Fig. 14. Automated right lane change simulation.

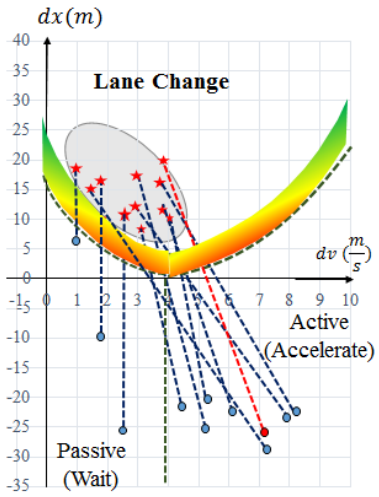

Fig. 15. dx/dv graph related to simulated right lane change scenario

proposed method with different initial (dx_{t_0}, dv_{t_0}) and the results are shown by dotted lines in Fig. 15. The tested results show that the proposed model works properly, without any collision during the lane change simulation.

B. *Merge and Exit*

The proposed dx/dv model was extended to cover more complicated cases of lane change for merging into traffic highway. In these cases, the time/ distance for doing lane change is limited. The suitable behaviors for merge and exit are active model (*accelerate* or *decelerate)* to do the lane change as soon as possible. The proposed dx/dv segments and suitable behavior for each segment is shown in Fig. 16. Two simulations to merge or exit (Fig. 17 and Fig.18) which consider two initial statuses for (dv, dx) are shown by LC_{006}, LC_{007} in Fig. 16. For LC_{006}, the value of (dv, dx) falls in the accelerate area and the acceleration behavior is selected to merge the expressway. For LC_{007}, the value of (dv, dx) falls in the deceleration area and the suitable behavior is decelerate to merge the expressway. As shown in Fig. 16, the dx/dv changes are not linear like normal lane changes and there are sharp changes in the dv (accelerate and decelerate) to enter the lane change area in shorter time. The simulation results for LC_{006}, LC_{007} are shown in the Fig. 18

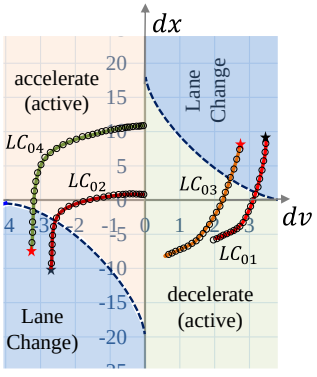

Fig. 16. dx/dv graph for right lane change simulation scenarios

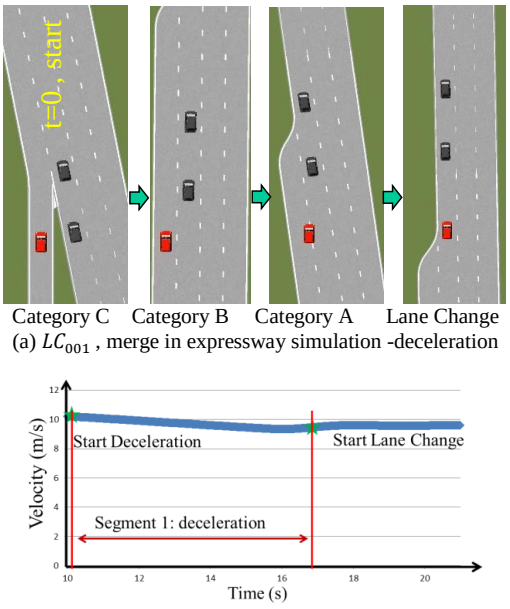

(a) LC_{001} , merge in expressway simulation -deceleration

(b) Velocity profile to merge into highway for LC_{001}

Fig. 17. Simulation results to merge into highway for LC_{001}.

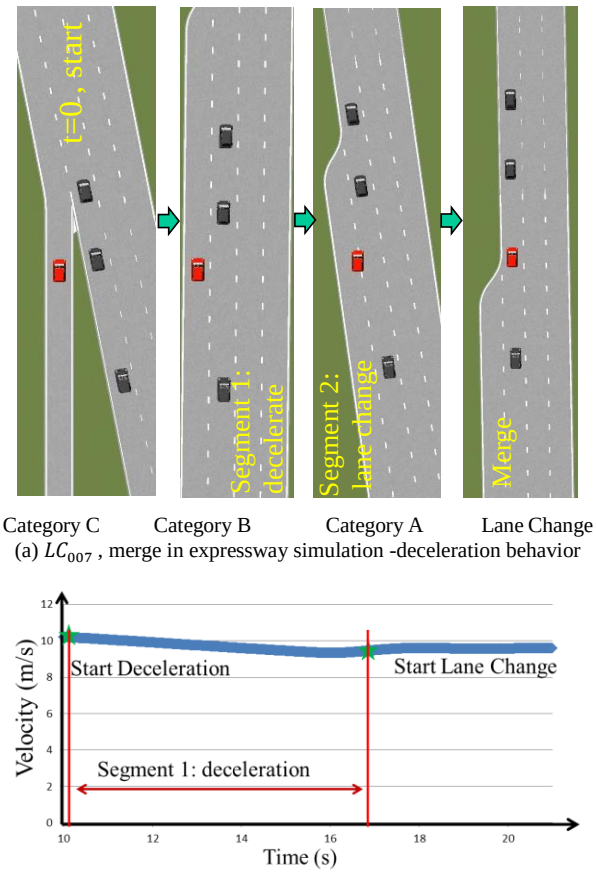

(a) LC_{007} , merge in expressway simulation -deceleration behavior

(b) Velocity profile

Fig. 18. Lane change simulation to merge.

(a), (b) respectively.

Simulations to exit the expressway are also carried out. Two examples which considering two initial statuses that are shown

by LC_{008}, LC_{009} in Fig. 16. In these case, there are also sharp changes in the dv (accelerate and decelerate) to enter the lane change area in shorter time. Based on the position in a prior known (or recorded global map), the ego vehicle is able to know if it is close to the merge or exit position or not. The system is then able to decide between patterns in Fig.9 or Fig.16.

C. Comparison between Human and Computer

In our method, we "mimic" the human driver in "behavior segment", however, in "motion segment", we applied polynomial functions to generate lane change trajectory. In this section, we compare human-driver with computer motion generator for "*motion segment*" during the expressway lane change. To evaluate both lateral and longitudinal trajectories in same function, the lateral jerk and smoothness are utilized as Kanayama and Hartman proposed [39]. Evaluation function is defined as integral over the square of arc-length derivative of curvature along the path for a function $f(x)$ with curvature $\kappa(x)$. The results of comparison between human-driver and computer motion generation for motion segment are shown in Table I. In most cases the computer can generate close or even better motion sets compared to human-driver (lower lateral jerk and lower smoothness^{-1}). The motion curvature $\kappa(t)$ of one lane change sample for computer motion generated and human-driver is shown in Fig. 19. As shown in this sample, the computer generated smoother motion (lower curvature) compared to human-driver.

TABLE I. COMPUTER AND HUMANI DRIVER ANALYSIS FOR LANE CHANGE DATA

Case	Operation Time -Δt (s)		Smoothness^{-1} $\int_0^T \frac{\kappa(t)^2}{\sqrt{\dot{x}(t)^2+\dot{y}(t)^2}}$		Lateral Jerk $\int_0^T \dddot{y}^2(t)$	
	Human-driver	Computer	Human-driver	Computer	Human-driver	Computer
1	4.92	5.075	1.23E-07	1.19E-07	0.746	0.761
2	7.135	7.175	1.12E-06	7.35E-07	0.810	0.802
3	4.195	4.06	8.35E-07	6.12E-07	1.280	1.145
4	4.265	4.22	4.00E-07	2.93E-07	2.275	2.102
5	4.15	4.17	7.34E-07	4.91E-07	0.432	0.303
6	3.66	3.705	3.10E-07	1.89E-07	1.306	1.022
7	3.02	3.075	9.70E-08	6.48E-08	0.229	0.199
8	3.995	4.04	3.19E-07	2.02E-07	1.049	0.863
9	5.605	5.6	8.94E-07	6.69E-07	1.859	1.463
10	4.285	4.315	3.94E-08	2.09E-08	0.351	0.205
11	3.195	3.18	2.37E-07	1.18E-07	0.334	0.242
12	3.025	3.02	3.09E-06	3.14E-06	6.611	8.112
13	4.83	4.965	3.22E-07	6.32E-08	0.573	0.130
14	3.85	4.1	1.46E-06	1.04E-06	4.226	3.823
15	4.585	4.665	2.62E-06	3.01E-06	10.156	12.169
16	5.155	4.96	1.23E-07	8.44E-08	0.760	0.597
17	4.335	4.545	1.79E-07	4.50E-08	0.473	0.205
18	4.425	4.375	1.01E-07	3.61E-08	0.475	0.186

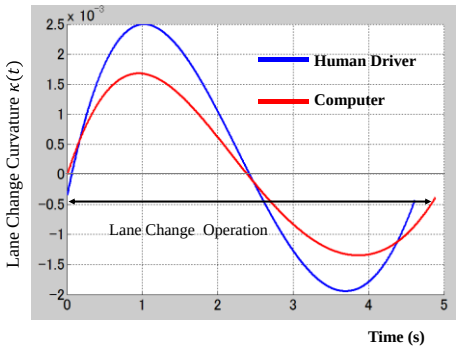

Fig. 19. Human-driver and computer curvature $\kappa(t)$ over time for lane change- blue curve shows smoothed IMU data from driver, red curve shows the computer

V. CONCLUSIONS

In this paper, a behavior/motion model for automated lane change at expressway has been proposed. The proposed model is mainly inspired by human-driver lane change and behavior data that can handle difficult lane change scenarios. The occupancy grid states are categorized and alternative behaviors are defined for each corresponding category. To select the suitable behavior, dx/dv graph is segmented based on the human-driver lane change patterns. Our experiments were carried on at the expressway where the lanes have different ranges of velocity. In this case, change to left or right lane means change to slower or higher speed lane. Thus, the segmented dx/dv will be dependent on the left or right lane change. The proposed model is intuitive and able to handle complicated lane change scenarios even in the presence of disturbances or sudden changes in behavior of surrounding vehicles. In future research, more human-driver lane change patterns are going to be extracted for better segmentation of dx/dv graph. Our current behavior model does not consider the interaction between the vehicles so that in future work, our model will consider it.

REFERENCES

[1] Volvo Trucks, European Accident Research and Safety Report.[Online]http://www.volvotrucks.com/SiteCollectionDocuments/VTC/Corporate/Values/ART%20Report%202013_150dpi.pdf, 2013.

[2] L. Fletcher et al. (2009), *The DARPA Urban Challenge, volume 56 of Springer Tracts in Advanced Robotics*, pp. 509–548. Springer Berlin Heidelberg.

[3] W. He, X. Wang, G. Chen, M. Guo, T. Zhang, P. Han and R. Zhang," Monocular based lane-change on scaled-down autonomous vehicles," in Proc. IEEE Intelligent Vehicles Symposium (IV), 2011, pp.144-149.

[4] W. Dolan and B. Litkouhi , "A prediction- and cost function-based algorithm for robust autonomous freeway driving," in *Proc. IEEE Intelligent Vehicles Symposium (IV)*, 2010, pp. 512–517.

[5] D. Kasper, G. Weidl, T .Dang, et al., "Object-Oriented Bayesian networks for detection of lane change maneuvers," *Intelligent Transportation Systems Magazine*, Vol. 4, No. 1, 2014, pp.19-31.

[6] D. Kasper, G. Weidl, T .Dang, et al., "Object-Oriented Bayesian networks for detection of lane change maneuvers," in *Proc. IEEE Intelligent Vehicles Symposium (IV)*, 2010, pp.673-678

[7] R. Schubert, K. Schulze, and G. Wanielik. (2010). Situation assessment for automated lane-change maneuvers. *IEEE Transactions on Intelligent Transportation Systems*, vol. 11, no. 3, pp. 607-616.

[8] S. Sivaraman and M. M. Trivedi, "Dynamic probabilistic drivability maps for lane change and merge driver assistance," *IEEE Transactions on Intelligent Transportation Systems*, vol.15, pp. 2063– 2073, 2014.

[9] R.S. Tomar, S. Verma, G.S. Tomar, "Prediction of lane change trajectories through neural network," in *Proc of International Conference on Computational Intelligence and Communication Networks*, 2010, pp. 249 – 253.

[10] A. Polychronopoulos, M. Tsogas, A. Amditis, et al, "Dynamic situation and threat assessment for collision warning systems: the euclide approach," in *Proc. IEEE Intelligent Vehicles Symposium (IV)*, 2004, pp. 636-641.

[11] T. Gindele, S. Brechtel, R. Dillmann, "A probabilistic model for estimating driver behaviors and vehicle trajectories in traffic environments," in *Proc International IEEE Conference on Intelligent Transportation Systems*, 2010, pp.1625-1631.

[12] J. Schlechtriemen, A. Wedel, J. Hillenbrand, G. Breuel, K. Kuhnert," A lane change detection approach using feature ranking with maximized predictive power", in *Proc. IEEE Intelligent Vehicles Symposium (IV)*, 2014, pp.108-114.

[13] J. Schlechtriemen, F. Wirthmueller, A. Wedel, G. Breuel, K. D. Kuhnert," When will it change the lane? a probabilistic regression approach for rarely occurring events," in *Proc. IEEE Intelligent Vehicles Symposium (IV)*, 2015,pp.1373-1379.

[14] P. Kumar, M. Perrollaz, S. Lef`evre, and C. Laugier," Learning-based approach for online lane change intention prediction," in *Proc. IEEE Intelligent Vehicles Symposium (IV)*, 2013, pp.797-802.

[15] E. Naranjo, C. Gonzalez, R. Garcia, and T. de Pedro, (2008). Lane-change fuzzy control in autonomous vehicles for the overtaking maneuver. *IEEE Transactions on Intelligent Transportation Systems*, vol. 9, no. 3, pp. 438-450.

[16] M. Bahram, A. Wolf, M. Aeberhard and D. Wollherr," A prediction-based reactive driving strategy for highly automated driving function on freeways ," in *Proc. IEEE Intelligent Vehicles Symposium (IV)*, 2014, pp.400-406.

[17] J. Nilsson and J. Sj¨oberg," Strategic decision making for automated driving on two-lane, one way roads using model predictive control," in *Proc. IEEE Intelligent Vehicles Symposium (IV)*, 2013,pp.1253-1258.

[18] Y. Du, Y. Wang and C. Chan," Autonomous lane-change controller via mixed logical dynamical", in *Proc . 17th International Conference on Intelligent Transportation Systems*, 2014, pp 1154 – 1159.

[19] Y. Du, Y. Wang and C. Chan," Autonomous lane-change controller", in *Proc. IEEE Intelligent Vehicles Symposium (IV)*, 2015, pp.386-393.

[20] U. Simon, and M. Markus, "Probabilistic online POMDP decision making for lane changes in fully automated driving," in *Proc of IEEE Conference on Intelligent Transportation Systems*, 2013, pp.2063-2070.

[21] S. Brechtel, T. Gindele, and R. Dillmann, "Probabilistic MDP-behavior planning for cars," in *Proc of 14th International IEEE Conference on Intelligent Transportation Systems*, 2011, pp.1537-1542.

[22] M. Ardelt, C. Coester, and N. Kaempchen. (2012). Highly automated driving on freeways in real traffic using a probabilistic framework. *IEEE Transactions on Intelligent Transportation Systems*, vol. 13, no. 4, pp. 1576-1585.

[23] Q. Jin, G. Wu, K. Boriboonsomsin, and M. Barth," Improving traffic operations using real-time optimal lane selection with connected vehicle technology," in *Proc. IEEE Intelligent Vehicles Symposium (IV)*, 2014,pp.70-75.

[24] H. Jula, E. Kosmatopoulos and P. Ioannou. (2000). Collision avoidance analysis for lane changing and merging. *IEEE Transactions on Vehicle Technology*, vol. 49, pp.2295 -2308.

[25] C. Rodemerk, S. Habenicht, A. Weitzel, H. Winner and T.Schmitt," Development of a general criticality criterion for the risk estimation of driving situations and its application to a maneuver-based lane change assistance system," in *Proc. IEEE Intelligent Vehicles Symposium (IV)*, 2012, pp.264-269.

[26] G.Schildbach, F. Borrelli, "Scenario Model Predictive Control for Lane Change Assistance on Highways", in *Proc of IEEE Intelligent Vehicles Symposium*, 2015, pp.611-616.

[27] J. Ziegler, P. Bender, T. Dang and C. Stiller, "Motion planning for Bertha - a local, continuous method," in *Proc of Intelligent Vehicles Symposium*, Dearborn, Michigan, USA, 2014, pp. 450-457.

[28] Q. H. Do, L. Han, H. Tehrani and S. Mita, "Safe path planning among multi obstacles," in *Proc of IEEE Intelligent Vehicles Symposium*, 2011, pp. 332 – 338.

[29] H. Tehrani, K. Muto, K. Yoneda and S. Mita, "Evaluating human & computer for expressway lane changing," in *Proc of IEEE Intelligent Vehicles Symposium*, 2014, pp. 382 – 387.

[30] Q. H. Do, H. Tehrani, M. Egawa, K. Muto, K. Yoneda, and S. Mita, "Distance constraint model for automated lane change to merge or exit," in *Proc of the 3rd International Symposium on Future Active Safety Technology Towards zero traffic accidents*, 2015, pp. 17-24.

[31] California Driver Handbook-Safe Driving Practices: Merging and Passing, California Department of Motor Vehicles, Sacramento, CA, USA,2012.

[32] W. Yao, H. Zhao, F. Davoine, H. Zha," Learning lane change trajectories from on-road driving data," in *Proc. IEEE Intelligent Vehicles Symposium (IV)*, 2012, pp.885-890.

[33] M. Werling, J. Zeigler, S. Kammel, S. Thrun, "Optimal trajectory generation for dynamic street scenarios in a Frenet Frame," in *Proc of IEEE International Conference on Robotic and Automation*, 2010, pp. 987-993.

[34] D. Althoff, M. Buss, A. Lawitzky, M. Werling, D. Wollherr "On-line trajectory generation for safe and optimal vehicle motion planning," AMS 2012, pp. 99-107.

[35] T. Fraichard and H. Asama. (2004). Inevitable Collision States. A step towards safer robots?. *Advanced Robotics*, vol. 18, pp. 1001–1024.

[36] H. Tehrani, Q. H. Do, M. Egawa, K. Muto, K. Yoneda, and S. Mita, "General behavior and motion model for automated lane change," in *Proc of IEEE Intelligent Vehicles Symposium*, 2015, pp. 1154-1159.

[37] L.Peng, A. Kurt, U. Özgüner ,"Trajectory prediction of lane changing vehicle based on driver behavior estimation and classification," in *Proc of Intelligent Transportation Systems*, 2014 , pp. 942 – 947.

[38] A A. Geiger, M. Lauer, F. Moosmann, B. Ranf et al. (2012). Team AnnieWAY's Entry to the 2011 Grand Cooperative Driving Challenge. *IEEE Transactions on Intelligent Transportation Systems*, vol 13, no 3, pp. 1008 – 1017.

[39] Y. Kanayama, G. R. De Haan," Least Cost Paths With Algebraic Cost Functions", in *Proc. IEEE International Workshop on Intelligent Robots*, 1988, pp.341-346.

Quoc Huy Do received his B.S. and M.S. degrees in Information Technology from Hanoi University of Technology, Vietnam, in 2006 and 2008, respectively. He served on the faculty of Hanoi University of Science and Technology in the academic years of 2006–2009. He received his Ph.D in information and systems from Toyota Technological Institute (TTI) in 2013. Currently, he is a post-doctoral fellow at Research Center for Smart Vehicles of TTI. His research field is path planning, vehicle dynamic and automated lane change for autonomous vehicles.

Hossein Tehrani Nik Nejad received his B.S. and M.S. degrees in industrial engineering from Sharif University of Technology, Iran, in 1996 and 1998, respectively. He received his Ph. D degree in mechanical engineering from Osaka Prefecture University, Japan, in 2009. In 2009, he joined the Toyota Technological Institute at Japan as Post-doctoral Fellow in the Smart Vehicle Center. In 2012, he joined the DENSO CORPORATION. Dr. Tehrani is an IEEE member and also a technical committee member of ITS-Nagoya chapter. His research interests are automated driving, sensor processing, machine learning and deep neural networks.

Seiichi Mita received his B.S., M.S., and Ph.D. degrees in electrical engineering from Kyoto University in 1969, 1971, and 1989, respectively. He studied at Hitachi Central Research Laboratory, Kokubunji, Japan, from 1971 to 1991, investigating signal processing and coding methods. Currently, he is a professor at Toyota Technological Institute (TTI) in Nagoya (since 1999) and a director of the Research Center for Smart Vehicles at TTI. Currently, he is greatly interested in the research area of autonomous vehicles and sensing systems. Dr. Mita is a member of the Institute of Electronics, Information and Communication Engineers and the Institute of Image Information and Television Engineers in Japan. He is also a member of IEEE. He received the best paper award from the IEEE Consumer Electronics Society in 1986 and the best paper and author awards from the Institute of Television Engineers in Japan in 1987 and 1992, respectively.

Kenji Muto received the M.S. degree in Electronic-Mechanical Engineering from Nagoya University in 1997. He currently works for research and development department in DENSO CORPORATION. His research interests have been in vehicular sensing and communication system and its applications.

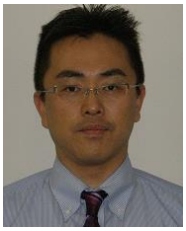

Masumi Egawa received his the B.E. and M.S. degrees from Nagoya Institute of Technology, in Nagoya, Japan, in 1996 and 1998 respectively. He currently works for DENSO CORPORATION.
His research interests have been in information security, wireless communication, and applications of machine learning methods

Keisuke Yoneda received his B.S. degrees in engineering from Toyohashi University of Technology in 2007, and M.S., and Ph.D. degrees in information science from Hokkaido University in 2009 and 2012, respectively. He is currently work as Assistant Professor at Autonomous Vehicle Research Unit of Institute for Frontier Science Initiative, Kanazawa University. He is interested in the research area of autonomous vehicles, artificial intelligence and artificial life. He is a member of the Japan Society for Precision Engineering and the Society of Automotive Engineers of Japan, Inc